

<https://doi.org/10.1038/s43247-025-02334-w>

Stability of aqueous neodymium complexes in carbonate-bearing solutions from 100–600 °C

Check for updates

Margaret E. Reece^{1,2}✉, Artas A. Migdisov¹, Anthony E. Williams-Jones³, Andrew C. Strzelecki¹, Laura Waters⁴, Hakim Boukhalfa¹ & Xiaofeng Guo²

Rare earth element exploration requires a quantitative understanding of factors governing their mobilization and economic concentration. However, the behavior of rare earth elements in carbonate-bearing hydrothermal fluids associated with carbonatite-hosted deposits is poorly understood, and conflicting mechanisms of rare earth transport by anionic ligands and alkali behavior have been described. Here, we report quantitative data to characterize the role of carbonate-bearing solutions in the hydrothermal mobilization of neodymium. Solubility studies of neodymium phosphate were performed at temperatures ranging from 100 to 600 °C in carbonate-bearing solutions. The thermodynamic data determined for the predominant complex were used to model the separation of neodymium from thorium in a simple flow-through system based on fluid and mineral compositions characteristic of carbonatite deposits. Our data suggest that neodymium transport is controlled by the stability of the carbonate species NdCO_3OH^0 , and at temperatures of 500–600 °C, the concentrations of neodymium in solutions can reach ~1000 ppm.

The twenty-first century has seen a mounting interest in the rare earth elements (REE) owing to their use in critical technologies that have become ubiquitous in the modern world¹. Unfortunately, the supply of these elements is not keeping up with their demand due to the shortage of economically extractable REE resources controlled by a small number of countries. Thus, identifying new REE resources is a high priority. There is general agreement that both magmatic and hydrothermal processes contribute heavily to the concentration of the REE to form ore deposits^{2–4}. Indeed, many REE deposits are either substantially hydrothermal in origin or have been enriched to economic concentrations by hydrothermal fluids^{5–8}. They are hosted dominantly by igneous intrusions and carbonatites, with the richest deposits being carbonatite-associated, e.g., Bayan Obo (China) and Mountain Pass (United States)^{9–16}. Studies of fluid inclusions from carbonatite deposits have documented a diverse range of salinity and ligand variety¹⁷. The most- and best-understood deposits from the perspective of REE transport and deposition, however, are those hosted by alkaline silicate rocks, e.g., the Strange Lake deposit (Canada), for which there is compelling evidence that the REE were transported in acidic solutions, likely as chloride complexes¹⁸. There is a general understanding of the transport and deposition of REE by acidic solutions in silicate-associated systems^{19,20}. However, there is very little information on their behavior in the higher pH carbonate-bearing hydrothermal systems that are responsible for

the formation of carbonatite-hosted REE deposits^{21–25}. Commonly reported brine solutions include alkali-chloride-(bi)carbonate ligand mixtures that are homogenized at temperature ranges from 100–800 °C²⁶. Given the importance of carbonate ions in such systems and the preference of the REE for hard ligands²⁷, it is reasonable to assume that REE transport and concentration in carbonatite-associated REE depositing hydrothermal systems depend on the stability of the REE-carbonate complexes in aqueous fluids and melt phases, the properties of which are largely unknown.

Aqueous complexes of REE that are expected to dominate solutions include chlorides, sulfates, and, more recently carbonates^{19,28}. Carbonate complexes are among the most stable REE-complexes at ambient conditions especially in solutions of moderate to high pH^{29,30}, but their stability at elevated P-T conditions is limited to theoretical predictions by Haas et al.³¹ and Wood³², which disagree by several orders of magnitude. Recent contributions by Yuan et al.²⁴ and Anenburg et al.²³ have enhanced the identification of the roles of alkalis in REE mobilization in carbonatitic melts or highly evolved melt-brines in addition to the qualitative study by Louvel et al.²² that revealed carbonate complexation in hydrothermal fluids can be achieved. Here, we investigate the mechanisms of REE transport in solutions that correspond with the conventional aqueous hydrothermal fluid categories and the influence of sodium chloride and carbonate ligands.

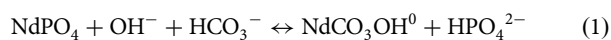
¹Los Alamos National Laboratory, Los Alamos, NM, USA. ²Washington State University, Pullman, WA, USA. ³McGill University, Montreal, QC, Canada. ⁴New Mexico Institute of Mining and Technology, Socorro, NM, USA. ✉e-mail: mreece@lanl.gov

This is the second in a series of investigations initiated that has focused on a quantitative evaluation of the effects of carbonate and salinity on the best-studied REE in terms of hydrothermal complexation, neodymium (Nd). The first study in this program was that of Nisbet et al.²¹, which had shown, at least up to 250 °C, that the transport of Nd in carbonate-bearing solutions is controlled overwhelmingly by carbonate complexes and that the stoichiometry of these complexes corresponds to either NdCO_3^+ (acidic solutions) or NdCO_3OH (alkaline solutions). Unfortunately, owing to the lack of thermodynamic data for Nd-hydroxylbastnäsite (which was the reference phase in the study of Nisbet et al.²¹), the absolute thermodynamic stability of these aqueous complexes was not determined and, thus, accurate modeling and prediction of the high-temperature behavior of Nd-carbonate complexes were not possible. The primary purpose of the current study, therefore, was to conduct experiments that would help quantify the mobilization of Nd by carbonate-bearing solutions in equilibrium with synthetic NdPO_4 at temperatures up to 600 °C. In natural systems, monazite, the natural analog for synthetic NdPO_4 , occurs as a solid solution. Since synthetic NdPO_4 has the same crystal structure as monazite, it is an excellent proxy for this mineral and can be used to reliably predict the behavior of monazite in the more complex natural systems.

Results

In the set of experiments, the solubility of synthetic NdPO_4 in aqueous solutions was determined as a function of A) carbonate concentration ranging from 0.005 to 0.5 m NaHCO_3 (or Na_2CO_3) with NaCl concentration constant for each given experimental temperature to satisfy the activity model described in the Supplementary Information File, and B) sodium chloride in concentrations from 0.1 to 2 m NaCl with a constant carbonate concentration. The first set of experiments was carried out at temperatures between 100 and 600 °C, and the second set at temperatures between 250 and 500 °C. The experiments employed autoclave (100–250 °C) and cold-seal (400–600 °C) solubility methods, which are described in more detail in the methods and materials section below and depicted in Supplementary Fig. S1.

The results of the solubility experiments are illustrated in Figs. 1 and 2. As can be seen in Fig. 1, which illustrates the concentration of dissolved Nd in the first set of experiments as a function of bicarbonate activity, each isotherm up to 400 °C is marked by an increase in the concentration of Nd with respect to the activity of bicarbonate in a ratio of 1:1. The pH dependence of these solutions (Supplementary Fig. S2) also exhibits a linear correlation of 1:1 and these data together support the stoichiometry determined by Nisbet et al.²¹ and indicate that the dominant complex controlling Nd solubility in alkaline solutions is NdCO_3OH^0 and that it forms via the following reaction:



We observed that at temperatures above 400 °C (Fig. 1), the solubility of the NdPO_4 increases sharply in agreement with Yuan et al.²⁴, even though carbornerite or bastnäsite was used in Yuan's experiment, and monazite is considered to be highly insoluble^{12,33}. In these higher temperature experiments, the PO_4^- buffer was exhausted and the otherwise linear relationship between the logarithms of the activity of bicarbonate and the measured molality of neodymium could not be applied. These results provide direct evidence of the efficiency with which carbonate complexes transport Nd, determined to be as high as 1000 ppm at 600 °C, in hydrothermal solutions.

The extremely high concentrations of Nd measured in our experiments at elevated temperatures cast serious doubt on the assumption that²³ alkalis and halogens are the dominating controls for hydrothermally mobilizing the REE in ore-forming concentrations. This hypothesis was evaluated with the help of the second set of experiments, in which NaCl was added in concentrations ranging from 0.1 to 2.0 m to solutions containing a fixed carbonate concentration at 250 °C, 400 °C and 500 °C. The results of these experiments are shown in Fig. 2. As is evident from the figure, the Nd concentration is effectively independent of the sodium chloride

concentration. In addition to the measured Nd concentrations, the figure also illustrates expected changes in the Nd concentration caused by the changing ionic strength of the solution based on the activity model. As can be seen, the predicted Nd concentrations agree remarkably well with the measured concentrations, emphasizing our conclusion that Nd solubility was not significantly increased by complexes involving Na or Cl. For details of the activity model, readers are referred to the Supplementary Information File.

The experimental data from the first set of experiments (Supplementary Table, S1) were used to calculate equilibrium constants, $\log K$ (Table 1), for Reaction (1) at each experimental temperature. Formation constants, $\log \beta$ (Table 1), relating the predominant species in solution, NdCO_3OH^0 , to the activity of Nd^{3+} and CO_3^{2-} were calculated using the following reaction:



For further information on the calculation of the formation constants, readers are referred to the Supplementary Information File.

Discussion

The high solubility of NdPO_4 at temperatures above 400 °C combined with the observations described by Yuan et al.²⁴ from different mineral reference phases supports the conclusion that carbonate has been underestimated as a transport ligand. The results of this study indicate that under the conditions of our experiments, aqueous Nd-carbonate complexes are extremely stable, and that the predominant species for alkaline conditions is the neutral complex, NdCO_3OH^0 . As shown previously by Nisbet et al.²¹, we found the contribution of Nd-chloride complexes to the total dissolved Nd concentration to be insignificant at the experimental conditions. These results also clearly demonstrate that the alkali metal sodium does not directly influence LREE mobility in hydrothermal fluids, however we do not exclude that both play some role in the mobilization of REE by carbonatitic melt-brines as demonstrated in Yuan et al.^{24,25}. Indeed, the presence of high concentrations of sodium chloride (up to 2 m) in one of our sets of experiments did not cause the dissolved neodymium concentration to deviate significantly from that predicted by the activity model. This supports our conclusion that carbonate is the principal ligand involved in mobilizing the LREE in carbonate-bearing hydrothermal fluids.

The data collected in this study support the conclusion of Louvel et al.²² that carbonate complexes are the main means by which the REE are mobilized in carbonate-bearing (alkaline) hydrothermal fluids. Our data suggest a considerably simpler stoichiometry for the predominant species (NdCO_3OH^0) than proposed by Louvel et al.²², whose study utilized XAS spectroscopy and identified closest atomic neighbors, the distances between which they optimized using density functional theory (DFT). This led them to conclude that the dominant REE species are $([\text{REE}_3(\text{CO}_3)_2(\text{OH})_4(\text{H}_2\text{O})_{12}]^+)$ and $([\text{REE}_3(\text{CO}_3)_3(\text{H}_2\text{O})_{12}]^{3+})$ for the REE = Gd or Yb. Given that the Nd:CO₃ ratio of 1:1 determined in our study is similar to the 3:2 or 3:3 ratios reported by Louvel et al.²², and that hydroxyl species are considered to participate in the complexes proposed in both studies, it is reasonable to conclude that similar REE complexes dominate solutions in the two studies.

While solubility techniques alone cannot differentiate a 1:1 from a 2:2 complex, the inability of water to support the favorable formation of the large or highly charged complexes proposed by Louvel et al.²² supports our conclusion that the dominant Nd species in our experiments was NdCO_3OH^0 . It is known that large or highly charged aqueous complexes, such as those proposed by Louvel et al.²² decrease in their relative stability with respect to neutral and simpler species at elevated temperatures. In part, this is because the kinetic motion of molecules makes complex structures less stable at elevated temperatures than species with simpler stoichiometry³⁴. Additionally, it is because the decrease in the dielectric constant of water with increasing temperature (e.g., from 80.1 at 20 °C to 7.2 at 373 °C at saturated vapor pressure)^{35,36} favors neutral and weakly charged ion pairs over highly charged complexes. Simply put, the breakdown of the

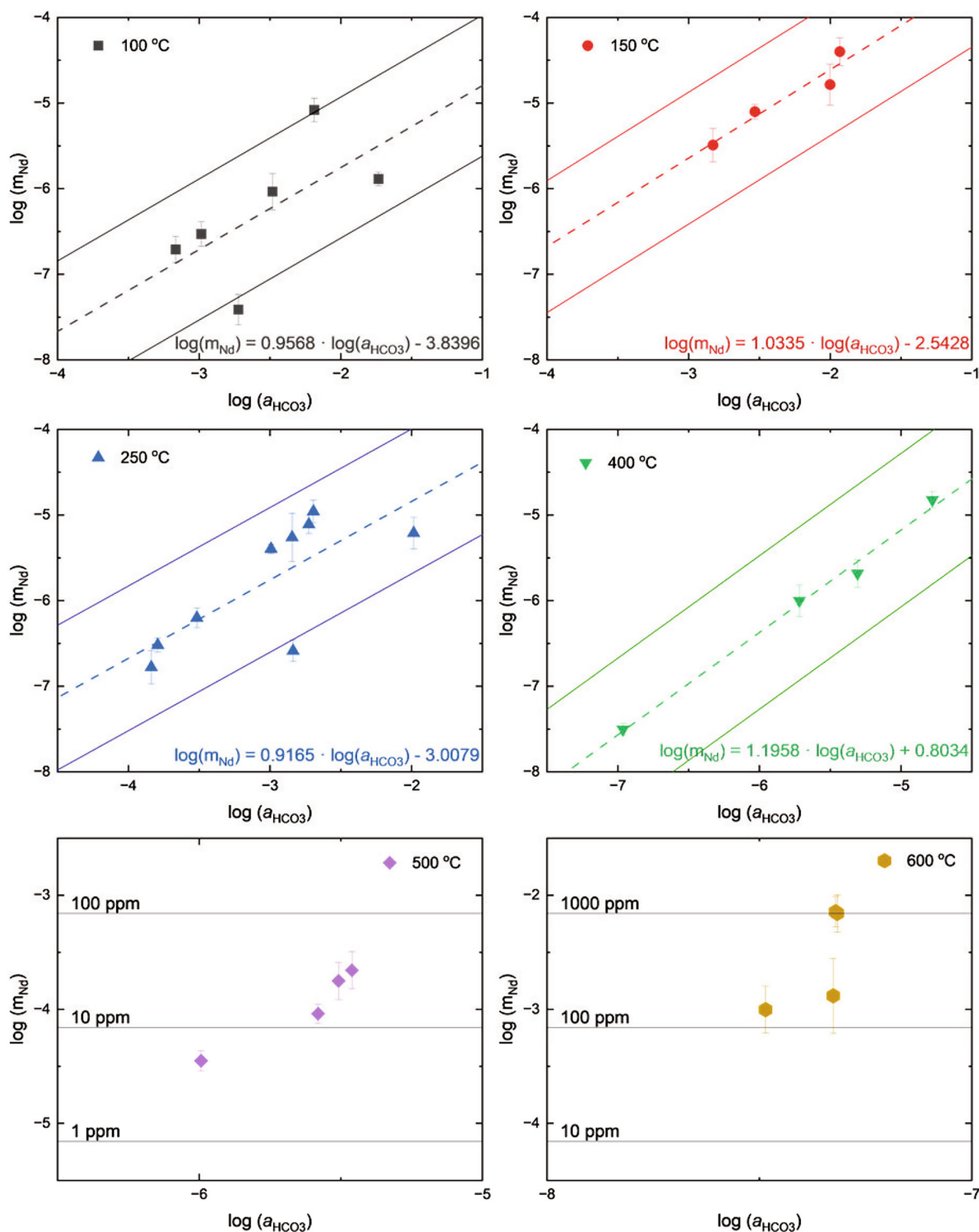


Fig. 1 | Solubility of Nd as a function of carbonate activity. Logarithms of the concentrations of Nd versus the logarithms of the calculated activity of HCO_3^- in solutions at 100 °C (gray squares), 150 °C (red circles), 250 °C (blue upward pointing triangles), 400 °C (green downward pointing triangles), 500 °C (purple diamonds), and 600 °C (gold hexagons) with errors propagated from the ICP-MS measurements. Linear fits (displayed with their 95% confidence error envelope as solid lines)

to the data were used to determine the dependence of Nd concentration on bicarbonate activity for temperatures up to 400 °C, whereas the data for 500 and 600 °C required numerical fitting individually by the model detailed in the Supplementary Information File. $[NaCl] = 1.0$ mol/kg for isotherms up to 400 °C and $[NaCl] = 0.5$ mol/kg in solutions at 500 and 600 °C.

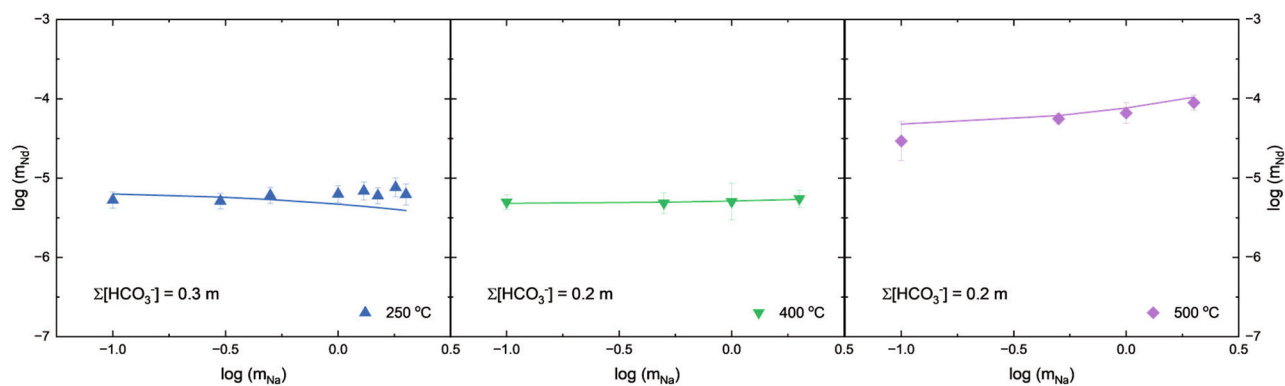


Fig. 2 | Solubility of Nd as a function of sodium chloride concentration. Logarithms of measured (symbols) and model-predicted (lines) Nd concentrations as a function of the logarithm of NaCl concentration in solution at 250 °C (left, blue), 400 °C (middle, green), and 500 °C (right, purple) with errors propagated from the ICP-MS measurements. The total HCO₃⁻ molality for each isotherm is indicated.

Table 1 | Thermodynamic constants. Calculated logarithms of equilibrium constants (log K) and formation constants (log β)

| Reaction | | Pressure | 100 °C | 150 °C | 250 °C | 400 °C | 500 °C | 600 °C |
|--|-------|-----------------|-------------|-------------|--------|--------|--------|-----------|
| NdPO ₄ + OH ⁻ + HCO ₃ ⁻ ↔ NdCO ₃ OH ⁰ + HPO ₄ ²⁻ | log K | Saturated vapor | -17.44 | -17.59 | -18.00 | | | |
| | | 1000 bar | | | | -17.90 | -17.43 | -15.61 |
| Nd ³⁺ + CO ₃ ²⁻ + H ₂ O ↔ NdCO ₃ OH ⁰ + H ⁺ | log β | Saturated vapor | 8.12 | 9.35 | 12.59 | | | |
| | | 1000 bar | | | | 16.03 | 20.56 | 26.42 |
| | | Uncertainty | ±0.37 | ±0.47 | ±0.54 | ±0.48 | ±0.51 | ±0.42 |
| Formation constants for other known Nd aqueous complexes | | | | | | | | |
| Reaction | log β | | | | | | | Reference |
| | 25 °C | 150 °C | 200 °C | 250 °C | | | | |
| Nd ³⁺ + Cl ⁻ ↔ NdCl ²⁺ | | 1.22 ± 0.21 | 2.25 ± 0.22 | 3.4 ± 0.25 | | | | 42 |
| Nd ³⁺ + 2 Cl ⁻ ↔ NdCl ₂ ⁺ | | | 3.15 ± 0.18 | 4.64 ± 0.21 | | | | |
| Nd ³⁺ + F ⁻ ↔ NdF ²⁺ | | 5.31 ± 0.21 | 6.11 ± 0.19 | 7.08 ± 0.20 | | | | 20 |
| Nd ³⁺ + SO ₄ ²⁻ ↔ NdSO ₄ ⁺ | 3.64 | | | | | | | 19 |
| Nd ³⁺ + 2 SO ₄ ²⁻ ↔ Nd(SO ₄) ₂ ⁻ | 5.15 | | | | | | | |

The equilibrium constants were calculated based on the tabulated reaction and are reported for each experimental temperature investigated together with the associated uncertainty. Formation constants of other available Nd aqueous complexes included for comparison^{19,20,42}.

hydrogen-bonded network of water molecules decreases the ability of this solvent to shield charged aqueous species^{35,36}, and, in turn, enhances ion pairing/association and promotes the stabilization of neutrally charged complexes^{22,37}.

The evidence provided in this study of the high propensity of carbonate-bearing fluids to mobilize REEs allows us to revisit the topic of the natural separation of REEs and associated radionuclides, such as thorium (Th) with thermodynamic data derived at the temperatures modeled below. Thorium commonly accompanies REEs in carbonate-bearing natural systems, not only as a constituent of the REE ores but also as a component of the minerals in the carbonatitic and alkaline silicate host rocks. The close association of Th with REE ores often poses a serious challenge for the REE mining industry due to the generation of radioactive waste streams. Therefore, identifying conditions under which Th-depleted REE ores can form is extremely important for REE exploration. Until now, the natural processes that efficiently separate REEs and Th in natural systems have not been reliably identified. The quantification of the high mobility of Nd in carbonate-bearing hydrothermal fluids and earlier findings demonstrating the extremely weak complexation of Th with carbonate³⁸ provide a hint to potential means of separating REEs from Th. To illustrate a possible mechanism for this separation, we developed a simple model, described in the Methods section below, simulating the flow of a hydrothermal fluid through rock.

There was an initial minor dissolution of thorianite from the wall rock that can be explained by the fact that these simulations were for alkaline conditions at which Th can form the stable Th(OH)₄⁰ complex³⁸. However, there was very limited mobilization of Th, whereas Nd remained in solution as the highly stable complex, NdCO₃OH⁰, until it precipitated as monazite (NdPO₄) at the end of the column (Fig. 3b–d). As the system evolved, a progressively higher proportion of Nd accumulated at the end of the column (in its low-temperature region). Although this process does not lead to the mobilization of Th from the wall rock, its relative concentration decreases systematically due to the accumulation of NdPO₄. It should be noted, however, that the model reported here is highly simplistic and is provided only for illustrative purposes. The precipitation of Nd was modeled through the formation of NdPO₄, as a proxy for monazite, whereas natural carbonate-enriched hydrothermal systems deposit a variety of other REE-bearing minerals, including fluorocarbonates, silicates and oxides. Similarly, the model does not consider Th-bearing minerals other than thorianite. Therefore, it should be used with caution, as the patterns of element mobility in natural systems are likely to be much more complex than that observed in this two-dimensional model. Nevertheless, the model does suggest how the REEs and Th may separate in rocks that have interacted with carbonate-bearing hydrothermal fluids. It should also be noted that the conclusions drawn in this study are only applicable to carbonate-rich systems, while

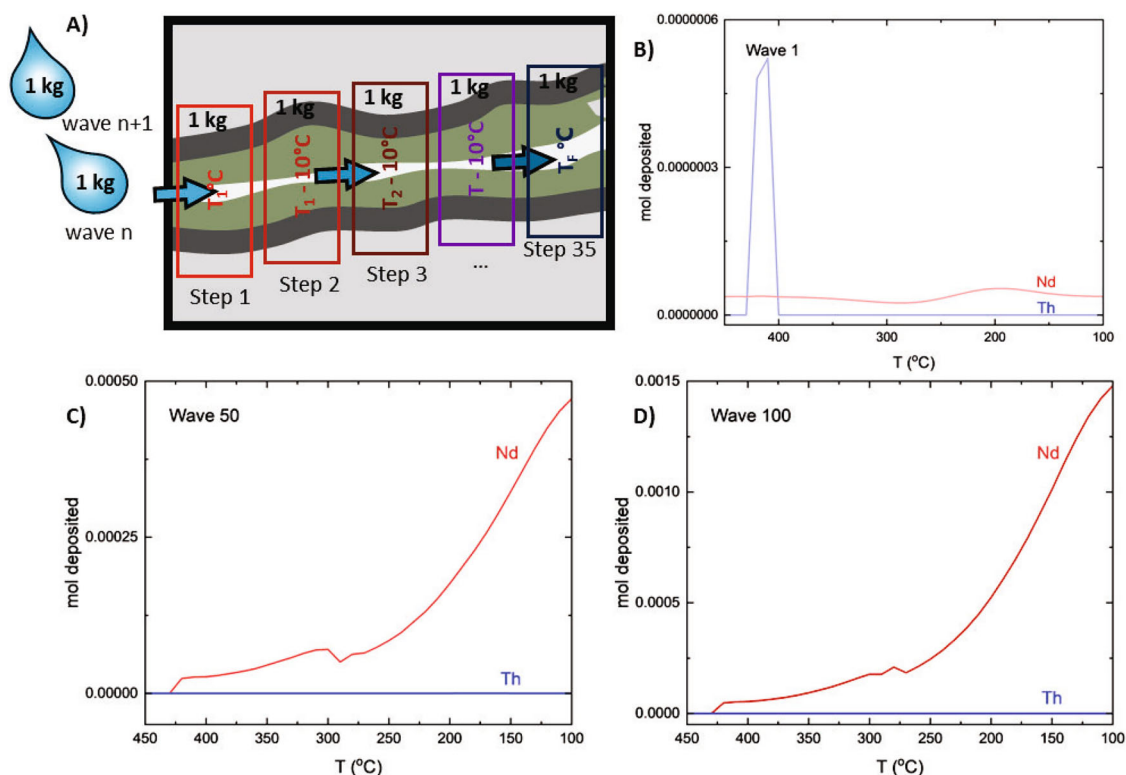


Fig. 3 | Redistribution of Nd and Th in a carbonate fluid column. A sketch of the model used to evaluate the fractionation of Nd from Th (A) and results of the flow-through simulation at wave 1 (B), wave 50 (C) and wave 100 (D). Each step lowered

the temperature of the column by 10°C . The accumulated Nd (as Nd-monazite) is shown in red, whereas the total Th (ThO_2 and Ca-Th-monazite) accumulated is shown in blue.

mobilization of rare earth elements in acidic media where carbonate is suppressed is dominated by chloride and sulfate complexes.

As mentioned in the introduction to this paper, the bulk of the World's REE resources are hosted by carbonatites, and in these rocks the REE were transported by carbonate-bearing hydrothermal fluids. Although the fluorocarbonate mineral, bastnäsite, is the principal ore mineral in most carbonatite-hosted or associated REE deposits, in a small number of them, monazite is the principal ore mineral. One of these deposits is the Ashram deposit (Canada)^{5,39}. Notably, the monazite in this deposit (it also contains subordinate bastnäsite) is Th-bearing and, moreover, the proportion of Th introduced into the monazite varied with the evolution of the system. This deposit, therefore, offers an excellent opportunity to test the REE-Th separation model developed here.

The Ashram deposit formed through the exsolution of fluids from a central breccia zone and evolved due to the interaction of these fluids with their dolomitic host rocks⁵. The key observation from the perspective of our box model is that the monazite which deposited furthest from the breccia has the highest REE and lowest Th content, whereas monazite deposited within the breccia or central conduit of the hydrothermal system has the lowest and highest contents of these elements respectively. Indeed, the Th content reaches 4.5 wt% in the monazite hosted by the breccia and is generally less than 0.3 wt% in the outer parts of the deposit. It is also noteworthy that the bastnäsite exhibits similar behavior. This shows clearly how the differential mobility of Th and the REE in carbonate-bearing hydrothermal fluids can lead to their effective separation in nature and, in turn, how the findings of this study can be used to guide the exploration for REE resources low in Th.

Conclusions

At temperatures up to 600°C , the dominant Nd species in carbonate-bearing alkaline solutions is NdCO_3OH^0 , and this species promotes the dissolution of NdPO_4 , resulting in the mobility of Nd in hydrothermal fluids. Moreover, the solubility of NdPO_4 directly increases with the activity

of carbonate at temperatures up to at least 600°C . The addition of NaCl to the fluid had no material effect on the mobility of Nd, showing that complexes involving Na do not mobilize Nd in alkaline carbonate-bearing fluids.

A simulation of the interaction of a Nd- and carbonate-bearing hydrothermal fluid with a column of carbonatite containing thorianite and apatite across a thermal gradient showed a considerable spatial separation of Nd from Th that increased with progressive fluid-rock interaction and decreasing temperature. This simulation reproduced the spatial separation that is observed between Th-rich and Th-poor monazite in the Ashram deposit, a large carbonatite-hosted REE deposit, and provided new insights into why this separation occurs and how low Th REE deposits can be successfully explored in the future.

Methods

Material synthesis and experimental setup

The experiments involved investigating the solubility of synthetic NdPO_4 (monazite) in aqueous fluids as a function of variable carbonate ($0.005\text{--}0.5\text{ m NaHCO}_3$ or Na_2CO_3) or sodium ($0.1\text{--}2.0\text{ m NaCl}$) concentrations at elevated temperatures ($100, 150, 250, 400, 500, 600^\circ\text{C}$). The reference Nd-monazite was synthesized by mixing equal volumes of aqueous solutions of NdCl_3 (0.2 M , Thermo Scientific, 99%) with Na_3PO_4 (0.25 M , J.T. Baker, >98%) and calcining the resulting precipitate at 900°C for 16 h. Experiments up to 250°C were carried out in Teflon-lined Ti autoclaves, whereas experiments at $400\text{--}600^\circ\text{C}$ were carried out in gold capsule cold-seal reactors. Solid reference phase material was placed in holders that prevented contact with the experimental solutions at ambient conditions. These holders were then placed into the reaction vessels with the reactant solution and sealed before being heated in a furnace for more than seven days. After heating, the reaction vessels were removed from the furnace and immediately quenched in a stream of cold air to room temperature in <25 min. The tubes containing the NdPO_4 were removed, and the resulting solution was acidified (H_2SO_4 , Fisher Scientific, TraceMetal Grade) and reheated to

200 °C to dissolve any Nd that may have precipitated on the walls during quenching. Finally, the concentration of Nd in the reacted solution was determined by Inductively Coupled Plasma-Mass Spectrometry (ICP-MS) at the Analytical Chemistry Laboratory of the New Mexico Institute of Mining and Technology. Sketches of the experimental setup are shown in (Supplementary Fig. S1).

Solubility experiments

The solutions for the first set of experiments, in which the impact of varying the carbonate concentration on Nd solubility was investigated, used solutions prepared with a constant NaCl (Fisher Scientific, A.C.S. Grade) concentration (1.0 or 0.5 m for a given T) and NaHCO₃ or Na₂CO₃ (J.T. Baker, >98%) concentrations varying from 0 to 0.5 molal. The experimental solutions for the second set of experiments in which the effect of sodium concentration on Nd solubility was investigated (0.1–2.0 m NaCl) were prepared with a carbonate concentration of 0.2–0.3 molal to ensure a constant HCO₃⁻ molality for all the experiments at each temperature. Synthetic Na₃PO₄ (Fischer Scientific, >98%) was added to all the experimental solutions in concentrations of 2.5–5.0 × 10⁻⁴ molal (constant for each isotherm) to control the phosphate buffering capacity of the solutions. The experimental parameters for each solution, including the calculated $a_{\text{HCO}_3^-}$ at the experimental temperatures, are reported in Supplementary Table S1.

The reference solid was characterized before experiments using X-ray diffraction (XRD, Bruker D2 Phaser, Supplementary Fig. S3) and Raman spectroscopy to ensure that the precursor had been completely converted to monazite. Raman spectroscopic analysis was also performed on the reference solid after the experiments to ensure that no additional phases formed during the experiments (Supplementary Fig. S4). The time required to attain equilibrium was determined for the most concentrated carbonate solutions to be ~5 days at 150 °C (Supplementary Fig. S5), and thus, we infer that the concentration of Nd achieved an equilibrium/steady state in all the experiments at T ≥ 150 °C (their duration was >7 days; the duration of the experiments at 100 °C was 16 days).

Separation model

This model comprises a simulation of the one-directional hydrothermal alteration of a column of rock containing thorianite (ThO₂) and apatite (Ca₁₀(PO₄)₆(OH)₂) by a fluid containing carbonate and Nd. The simulation used a step-flow reactor approach (box model, Fig. 3a), which involved the interaction and initial equilibration of the fluid with the rock at a pre-determined maximum temperature (450 °C, Step 1). The equilibrated fluid was then moved to the next reactor, where it equilibrated with unaltered rock at a lower temperature (Step 2). This was repeated until the temperature of the solution reached 100 °C. This column of rock with a temperature-gradient imposed in this manner, which was altered through its interaction with the first fluid aliquot (Wave 1), was then flushed with a fresh fluid aliquot of identical initial composition and allowed to equilibrate (Wave 2), thereby simulating the progressive evolution of the hydrothermal system. This process was repeated for a total of 100 waves, allowing us to predict how Th and Nd are likely to behave in well-evolved hydrothermal systems that experience continuous flushing by fluid. For a complete description of the model, readers are referred to the Supplementary Information File.

Data availability

All experimental data used to support the findings of this study are included in this article (and its Supplementary Information File).

Code availability

The HCh software package is a legacy product that was first described in 1999 and later expanded in 2015 and commercially distributed by Australia Geosciences^{40,41}. For questions regarding the current availability of this software, readers should contact those corresponding authors directly.

Received: 3 February 2025; Accepted: 24 April 2025;

Published online: 07 May 2025

References

- Schulz, K. J., DeYoung, J. H. Jr., Bradley, D. C. & Seal II, R. R. *Critical Mineral Resources of the United States - Economic and Environmental Geology and Prospects for Future Supply* (2017).
- Xie, Y. et al. A Model for Carbonatite Hosted REE Mineralisation — the Mianning–Dechang REE Belt, Western Sichuan Province, China. *Ore Geol. Rev.* **70**, 595–612 (2015).
- Bühn, B., Rankin, A. H., Schneider, J. & Dulski, P. The nature of orthomagmatic, carbonatitic fluids precipitating REE, Sr-rich fluorite: fluid-inclusion evidence from the Okorusu fluorite deposit, Namibia. *Chem. Geol.* **186**, 75–98 (2002).
- Veksler, I. V. Liquid immiscibility and its role at the magmatic-hydrothermal transition: a summary of experimental studies. *Chem. Geol.* **210**, 7–31 (2004).
- Beland, C. M. J. & Williams-Jones, A. E. The genesis of the Ashram REE deposit, Quebec: Insights from bulk-rock geochemistry, Apatite-Monazite-Bastnäsite replacement reactions and mineral chemistry. *Chem. Geol.*, **578**. <https://doi.org/10.1016/j.chemgeo.2021.120298> (2021).
- Vasyukova, O. V. & Williams-Jones, A. E. Closed system fluid-mineral-mediated trace element behaviour in peralkaline rare metal pegmatites: evidence from Strange Lake. *Chem. Geol.*, **505**. <https://doi.org/10.1016/j.chemgeo.2018.12.023> (2019).
- Cook, N. J. et al. Mineral chemistry of Rare Earth Element (REE) mineralization, Browns Ranges, Western Australia. *Lithos* **172–173**, 192–213 (2013).
- Smith, M. P., Campbell, L. S. & Kynicky, J. A. Review of the genesis of the world class Bayan Obo Fe-REE-Nb deposits, Inner Mongolia, China: Multistage processes and outstanding questions. *Ore Geol. Rev.*, **64**. <https://doi.org/10.1016/j.oregeorev.2014.03.007> (2015).
- Di, J. & Ding, X. Complexation of REE in hydrothermal fluids and its significance on REE mineralization. *Minerals*. Multidisciplinary Digital Publishing Institute (MDPI). <https://doi.org/10.3390/min14060531> (2024).
- Dostal, J. Rare metal deposits associated with alkaline/peralkaline igneous rocks. In *Rare Earth Crit. Elements Ore Deposits*. <https://doi.org/10.5382/rev.18.02> (2019).
- Cheng, Z., Zhang, Z., Aibai, A., Kong, W. & Holtz, F. The role of magmatic and post-magmatic hydrothermal processes on rare-earth element mineralization: a study of the Bachu carbonatites from the Tarim Large Igneous Province, NW China. *Lithos*, **314–315**. <https://doi.org/10.1016/j.lithos.2018.05.023> (2018).
- Sheard, E. R., Williams-Jones, A. E., Heiligmann, M., Pederson, C. & Trueman, D. L. Controls on the concentration of Zirconium, Niobium, and the rare earth elements in the Thor lake rare metal deposit, Northwest Territories, Canada. *Economic Geology*, **107**. <https://doi.org/10.2113/econgeo.107.1.81> (2012).
- Anenburg, M., Broom-Fendley, S. & Chen, W. Formation of rare earth deposits in carbonatites. *Elements*, **1**. <https://doi.org/10.2138/GSELEMENTS.17.5.327> (2021).
- Smith, M. P. & Henderson, P. Preliminary fluid inclusion constraints on fluid evolution in the Bayan Obo Fe-REE-Nb Deposit, Inner Mongolia, China. *Economic Geology*, **95**. <https://doi.org/10.2113/gsecongeo.95.7.1371> (2000).
- Kynicky, J., Smith, M. P. & Xu, C. Diversity of rare earth deposits: the key example of China. *Elements*, **8**. <https://doi.org/10.2113/gselements.8.5.361> (2012).
- Jaireth, S., Hoatson, D. M. & Mieziitis, Y. Geological setting and resources of the major rare-earth-element deposits in Australia. *Ore Geol. Rev.* <https://doi.org/10.1016/j.oregeorev.2014.02.008> (2014).
- Walter, B. F. et al. Fluids associated with carbonatitic magmatism: a critical review and implications for Carbonatite magma ascent. *Earth Sci. Rev.* **215**, 103509 (2021).
- Gysi, A. P. & Williams-Jones, A. E. Hydrothermal mobilization of Pegmatite-hosted REE and Zr at Strange Lake, Canada: A reaction

- path model. *Geochim. Cosmochim. Acta*, **122**. <https://doi.org/10.1016/j.gca.2013.08.031> (2013).
19. Migdisov, A. A., Williams-Jones, A. E., Brugger, J. & Caporuscio, F. A. Hydrothermal transport, deposition, and fractionation of the REE: Experimental data and thermodynamic calculations. *Chem. Geol.* <https://doi.org/10.1016/j.chemgeo.2016.06.005> (2016).
 20. Migdisov, A. A., Williams-Jones, A. E. & Wagner, T. An experimental study of the solubility and speciation of the Rare Earth Elements (III) in fluoride- and chloride-bearing aqueous solutions at temperatures up to 300 °C. *Geochim. Cosmochim. Acta*, **73**. <https://doi.org/10.1016/j.gca.2009.08.023> (2009).
 21. Nisbet, H. et al. The solubility and speciation of Nd in carbonate-bearing hydrothermal fluids up to 250 °C. *Chem. Geol.*, **611**. <https://doi.org/10.1016/j.chemgeo.2022.121122> (2022).
 22. Louvel, M., Etschmann, B., Guan, Q., Testemale, D. & Brugger, J. Carbonate complexation enhances hydrothermal transport of rare earth elements in alkaline fluids. *Nat. Commun.*, **13**. <https://doi.org/10.1038/s41467-022-28943-z> (2022).
 23. Anenburg, M., Mavrogenes, J. A., Frigo, C. & Wall, F. *Rare Earth Element Mobility in and around Carbonatites Controlled by Sodium, Potassium, and Silica*; **6**. <https://www.science.org> (2020).
 24. Yuan, X., Yang, Z., Mayanovic, R. A. & Hou, Z. *Experimental Evidence Reveals the Mobilization and Mineralization Processes of Rare Earth Elements in Carbonatites*; **10**. <https://www.science.org> (2024).
 25. Yuan, X., Zhong, R., Xiong, X., Gao, J. & Ma, Y. *Transition from Carbonatitic Magmas to Hydrothermal Brines: Continuous Dilution or Fluid Exsolution?*. <https://www.science.org> (2023).
 26. Rankin, A. H. Carbonatite-Associated Rare Metal Deposits: Composition and Evolution of Ore-Forming Fluids—the Fluid Inclusion Evidence. In *Rare-element geochemistry and mineral deposits: Geological Association of Canada, Short Course Notes* (eds Linnen, R. L. & Samson, I. M.) 299–314 (2005).
 27. Pearson, R. G. Hard and Soft Acids and Bases. *J. Am. Chem. Soc.*, **85**. <https://doi.org/10.1021/ja00905a001> (1963).
 28. Cantrell, K. J. & Byrne, R. H. Rare earth element complexation by carbonate and oxalate ions. *Geochim. Cosmochim. Acta*, **51**. [https://doi.org/10.1016/0016-7037\(87\)90072-X](https://doi.org/10.1016/0016-7037(87)90072-X) (1987).
 29. Elliott, H. A. L. et al. Fenites associated with carbonatite complexes: a review. *Ore Geol. Rev.* <https://doi.org/10.1016/j.oregeorev.2017.12.003> (2018).
 30. Johannesson, K. H., Stetzenbach, K. J. & Hodge, V. F. Speciation of the rare earth element Neodymium in groundwaters of the Nevada Test Site and Yucca Mountain and Implications for Actinide Solubility. *Appl. Geochem.*, **10**. [https://doi.org/10.1016/0883-2927\(95\)00028-3](https://doi.org/10.1016/0883-2927(95)00028-3) (1995).
 31. Haas, J. R., Shock, E. L. & Sassani, D. C. Rare earth elements in hydrothermal systems: estimates of standard partial molal thermodynamic properties of aqueous complexes of the rare earth elements at high pressures and temperatures. *Geochim. Cosmochim. Acta*, **59**. [https://doi.org/10.1016/0016-7037\(95\)00314-P](https://doi.org/10.1016/0016-7037(95)00314-P) (1995).
 32. Wood, S. A. The aqueous geochemistry of the rare-earth elements and Yttrium. 2. Theoretical predictions of speciation in hydrothermal solutions to 350 °C at saturation water vapor pressure. *Chem. Geol.* [https://doi.org/10.1016/0009-2541\(90\)90106-H](https://doi.org/10.1016/0009-2541(90)90106-H) (1990).
 33. Gysi, A. P., Harlov, D. & Miron, G. D. The solubility of Monazite (CePO₄), SmPO₄, and GdPO₄ in aqueous solutions from 100 to 250 °C. *Geochim. Cosmochim. Acta*, **242**. <https://doi.org/10.1016/j.gca.2018.08.038> (2018).
 34. Brugger, J. et al. A review of the coordination chemistry of hydrothermal systems, or do coordination changes make ore deposits? *Chem. Geol.* <https://doi.org/10.1016/j.chemgeo.2016.10.021> (2016).
 35. Uematsu, M. & Frank, E. U. Static dielectric constant of water and steam. *J. Phys. Chem. Ref. Data*, **9**. <https://doi.org/10.1063/1.555632> (1980).
 36. Fernández, D. P., Goodwin, A. R. H., Lemmon, E. W., Levett Sengers, J. M. H. & Williams, R. C. A formulation for the static permittivity of water and steam at temperatures from 238 K to 873 K at pressures up to 1200 MPa, including derivatives and Debye-Hückel coefficients. *J. Phys. Chem. Ref. Data*, **26**. <https://doi.org/10.1063/1.555997> (1997).
 37. Seward, T. M., Williams-Jones, A. E. & Migdisov, A. A. The chemistry of metal transport and deposition by ore-forming hydrothermal fluids. In *Treatise on Geochemistry: Second Edition*; **13**. <https://doi.org/10.1016/B978-0-08-095975-7.01102-5> (2014).
 38. Nisbet, H. et al. The solubility of Thorium in carbonate-bearing solutions at hydrothermal conditions. *Geochim. Cosmochim. Acta*, **330**. <https://doi.org/10.1016/j.gca.2021.04.035> (2022).
 39. Beland, C. M. J. & Williams-Jones, A. E. The mineralogical distribution of the REE in Carbonatites: A quantitative evaluation. *Chem. Geol.*, **585**. <https://doi.org/10.1016/j.chemgeo.2021.120558> (2021).
 40. Shvarov, Y. & Bastrakov, E. N. *HCh: A Software Package for Geochemical Modelling. User's Guide*; Record **25** (1999).
 41. Shvarov, Y. A Suite of Programs, OptimA, OptimB, OptimC, and OptimS Compatible with the Unitherm Database, for deriving the thermodynamic properties of aqueous species from solubility, potentiometry and spectroscopy measurements. *Appl. Geochem.*, **55**. <https://doi.org/10.1016/j.apgeochem.2014.11.021> (2015).
 42. Migdisov, A. A. & Williams-Jones, A. E. An experimental study of the solubility and speciation of Neodymium (III) Fluoride in F-bearing aqueous solutions. *Geochim. Cosmochim. Acta*, **71**. <https://doi.org/10.1016/j.gca.2007.04.004> (2007).
- ## Acknowledgements
- The research was supported by the U.S. Department of Energy, Office of Science, Office of Basic Energy Sciences, Geosciences program under award number DE-SC0022269 (awarded to A.A.M.) and the National Science Foundation, Division of Earth Sciences under award number 2149848 (awarded to X.G.). We also thank Bonnie Frey and Hannah Han at the Analytical Chemistry Laboratory at New Mexico Tech.
- ## Author contributions
- M.E.R., A.A.M., and A.W.-J. developed the ideas. M.E.R. prepared samples, conducted the Ti autoclave solubility experiments, performed the ICP-MS analysis, developed the model, and wrote the manuscript with input from all authors. M.E.R. and A.C.S. performed the XRD and Raman analysis for phase characterization. A.A.M. set up and performed the cold-seal solubility experiments and developed the model. L.W. and H.B. critically advised experimental setups. Critical revision was provided by A.W.-J. and funding was provided through A.A.M. and X.G.
- ## Competing interests
- The authors declare no competing interests.
- ## Additional information
- ### Supplementary information
- The online version contains supplementary material available at <https://doi.org/10.1038/s43247-025-02334-w>.
- ## Correspondence
- and requests for materials should be addressed to Margaret E. Reece.
- ## Peer review information
- Communications Earth & Environment* thanks Denis Testemale and Xueyin Yuan for their contribution to the peer review of this work. Primary Handling Editors: Carolina Ortiz Guerrero. A peer review file is available.
- ## Reprints and permissions information
- is available at <http://www.nature.com/reprints>
- ## Publisher's note
- Springer Nature remains neutral with regard to jurisdictional claims in published maps and institutional affiliations.

Open Access This article is licensed under a Creative Commons Attribution-NonCommercial-NoDerivatives 4.0 International License, which permits any non-commercial use, sharing, distribution and reproduction in any medium or format, as long as you give appropriate credit to the original author(s) and the source, provide a link to the Creative Commons licence, and indicate if you modified the licensed material. You do not have permission under this licence to share adapted material derived from this article or parts of it. The images or other third party material in this article are included in the article's Creative Commons licence, unless indicated otherwise in a credit line to the material. If material is not included in the article's Creative Commons licence and your intended use is not permitted by statutory regulation or exceeds the permitted use, you will need to obtain permission directly from the copyright holder. To view a copy of this licence, visit <http://creativecommons.org/licenses/by-nc-nd/4.0/>.

© The Author(s) 2025